Velocity and Turbulent Flow Field at Around the Cylindrical Pier

R. Karthik, U. Kumar, A.K. Barbhuiya

Abstract**:** ***This experimental study shows the velocity and turbulence field at vicinity of cylindrical pier with scour hole under clear water condition. The three dimensional velocity data were obtained at 5 cm, 10 cm, 20 cm and 30 cm from the pier with use of Acoustic Doppler Velocimeter at 360 degrees around the pier with 30-degree interval. The flow behaviour were extensively analyzed with the help of time averaged normalized velocity, Turbulent intensity, Turbulent kinetic energy and Reynolds shear stress plots. The study shows the flow behaviour at inside the scour hole, at scour hole ring and outside the scour hole which gives the elusive view of flow at vicinity of pier. An upstream side pier, the flow behaviour almost follows the similar trend but behind a cylinder the flow is asymmetry due to wake vortex and vortex shedding found at the wake region. This study offers an ample cognizance of flow structure at vicinity of circular pier, which is essential in order to design an effective scour control structures like rip-rap, W weir, vanes, slot and etc.,***

Keywords**:** ***ADV, Bridge, Flow measurement, Local scour, open channel, Pier***

I. INTRODUCTION

Bridge failure in the river is one of the generic and sensitive issues. On the testimony of [1]. Failures of bridges and offshore structures are mainly caused by local scour. The flow becomes complex and perturbated when it encountered a vertical obstruction. A large number of experiments were carried out to study the scour phenomena at bridge pier, and they developed an empirical relation for finding scour depth [2]. Prediction of scour depths by those available models is not always accurate due to the sparsity of knowledge of the flow features at the vicinity of piers [3], [4].

When flow met the obstruction, the downflow occurs at the front of, and the base of the pier; the vortex started to generate which is known as horseshoe vortex. The flow further goes into the downstream side, and a wake vortex occurs at a rear side of the pier which helps to keep the eroded particle into floating conation. Woke vortex also acts like a vacuum cleaner. The local scour developed at the vicinity of the stanchion of a bridge is mainly caused by the horseshoe vortex and wake vortex as articulated by [5].

The flow character at a vicinity of the pier was reported by many researchers in the past such as [6]–[13]and etc., [14] has studied the flow structure at two eccentric piers, [15]has compared the flow structures with circular and compound piers. [16], [17] studied the flow character at side by side piers and tandem piers. Some researchers have studied the flow filed around the pier numerically, among [18]–[21] etc.,

The scour depth predictions by existing models are may not always practical [22], the complete comprehension of flow structure at vicinity of bridge pier is lacking [15]. [3] To understand the scour mechanisms with apropos of flow and turbulent inside the scour hole is deficient. The previous researchers had measure the flow field in a particular region, [6] had measure the flow properties at 0 to 90 degree with 30 degree interval and [3] had taken the flow data at 0, 45 and 90 degrees to study the horseshoe effect. [14] Had studied the flow pattern from -90° to 90° with 45° interval, [4] has study the flow pattern with 30° from 0° to 180°. In this study the flow measurement were taken from 360° around the pier with 30° interval.

This experimental analysis was performed to get the detailed flow features like velocity and turbulence characteristics at inside, outside the scour hole at around the circular pier to an entire 360 degree. This detailed flow structure can give an insight to the designer, how the flow behaves at inside the scour hole and verge of scour hole ring when compared to outside the scour hole. Moreover better grasp of flow structure can helps the modelling the process of scour at vicinity of pier.

II. METHODS

The experimental runs were performed at a rectangular flume located in Hydraulic Engineering laboratory at NIT Silchar. The flume has a length of 20.45 m and cross-sectional size of 0.8 m width and 0.8 m depth. A perforated steel plate with the porosity of 0.7 covered the entire width, which is placed at the inlet of the flume to diminish the flow disturbances and stabilize the flow which entered into the flume.

Revised Manuscript Received on March 28, 2020.

***** Correspondence Author

R. Karthik*, Civil Engineering department, National Institute of Technology Silchar, Assam, India.

U. Kumar, Civil Engineering department, National Institute of Technology Silchar, Assam, India.

A.K. Barbhuiya, Civil Engineering department, National Institute of Technology Silchar, Assam, India.

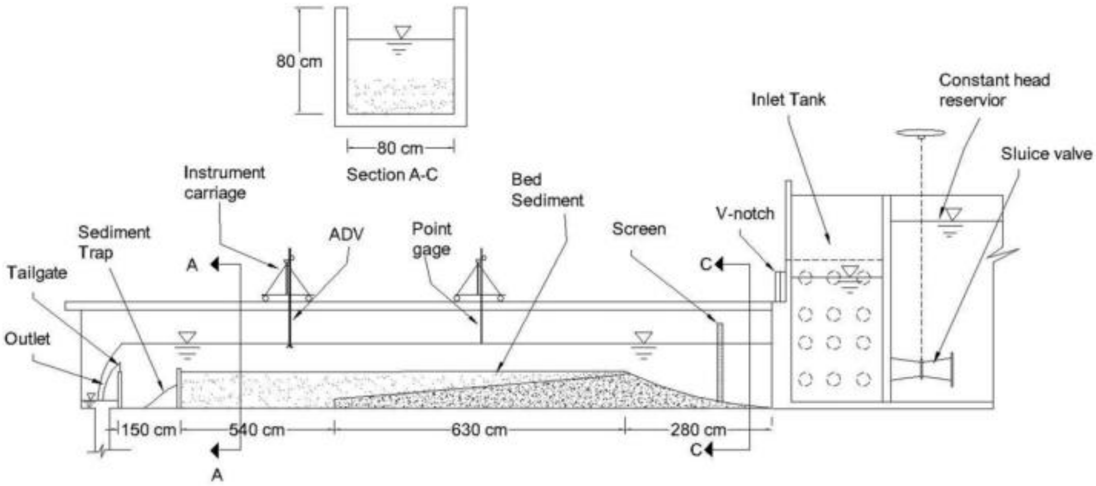

Fig.1. Schematic diagram of experimental set-up

The flume was filled up to 40 cm with a uniform sand particle having median size (d_{50}) and geometric standard deviation of particle distribution (σg) is 0.2 mm and 1.31 respectively. A gate valve can control the discharge of the flume, and the release of water is calculated by measuring the flow depth with point gauge at calibrated V notch. At the end of the flume, a sediment trap is provided to arrest those scoured particles. The flow depth was controlled by a tailgate which located at the end of the flume.

The pier of diameter 7.5 cm is made out of Perspex. At 7.5 m from the inlet, the cylinder was placed. The selected pier size is less than 10% of the width of the flume to reduce the blockage effects [23]. The flume is capable enough to generate 3-Dimensional flow; the flow is fully turbulent before it reaches the test location which is ensured by the formula of boundary layer thickness on smooth flat plate $\delta=0.37L_dUL_dv^{-0.2}$, Where, δ = thickness of Boundary layer, L_d = Distance along the streamwise direction.

The flume bed was levelled carefully before the experiment begins and the pier was placed on the centre of the flume at the test location. The thin sheet flow of water was allowed to pass through from the downstream end of the flume, to avoid the erosive action of water on a bed. The water was filled with low rate until it reached the desired depth; after that, the experiment will begin when the main pump is started. For clear water condition, the water is allowed to run up to 24 hours to reach the quasi-equilibrium scour as the maximum scour depth is exceeding more than 5mm after 24 hours performed by [24].

To achieve the clear water condition, the ratio of the shear velocity of approaching flow U^* to the critical shear velocity of sediment U^*_{cr} should be less than unity. To achieve the clear water condition U^*/U^*_{cr} was 0.67, the approaching flow velocity and depth is kept at 18.88 cm/s and 27.78 cm respectively. The velocity was measured around the pier with the 30˚ interval to understand the flow features at the vicinity of the pier. In each plane, the instantaneous velocity was measured at four locations, namely, at the scour hole, 10 cm, 20 cm and 30 cm from the pier with the help of Acoustic Doppler velocimeter (ADV).

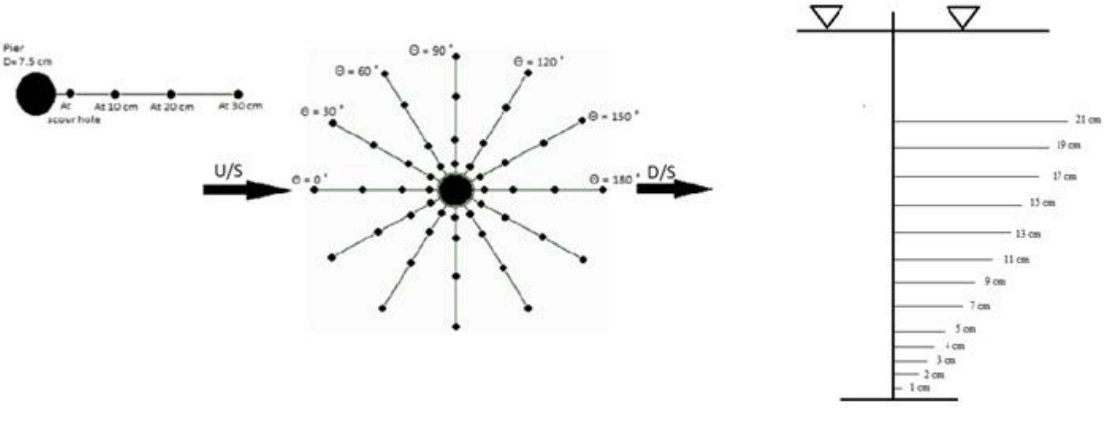

Fig.2. Detailed view of velocity measurement points.

In this study, 5 cm down-looking ADV from Sontek is used to obtain the 3-Dimensional instantaneous velocity. The ADV comprised of one transmitting unit which is located at the centre of the instrument and three receiving arms which are stationed at 120˚ each. The working principle of ADV is that the transmitting unit sends the acoustic signal which goes into the water and gets reflected by the ambient particles which present in the water and the reflected acoustic signal is received by receiving unit. The acoustic signals of ADV are processed by the processing module to measure the pulse-to-pulse Doppler shift to give the 3D instantaneous velocity.

Horizon ADV is the software provided by the Sontek, which helps to display the real-time three-dimensional instantaneous velocities along with mean correlation and the signal-noise ratio (SNR) with tabular and graphical form. The SNR value is decidedly less when the ADV is closer to the bed.

To obtain satisfactory data, the raw data of ADV has to perform the de-spiking to remove unwanted and inaccurate data. The de-spiking was done with the help of winADV software [25], [26] which was provided by the Bureau of Reclamation. To achieve the quality data, ADV standard SNR and mean correlation is kept as greater than 15 and greater than 70 and the data used in this study strictly followed the afore-mentioned criteria [27].

Once the scour profile reached the equilibrium, the pump stopped, and the water is allowed to be released from flume at a low rate without disturbing the scour profile. The instantaneous 3-Dimensional velocity was measured vertically from bed at every 1 cm up to 10 cm, and the rest of the flow depth was measured at every 2 cm. The velocity measurement up to 5 cm from free surface is not possible due to the limitation of ADV [28].

III. RESULTS AND DISCUSSION

The length of vertical measurements were normalized with flow depth and approaching flow velocity was normalized by mean approaching velocity, to get time-averaged normalized velocities. The velocity component u, v and w is longitudinal, lateral and vertical velocity respectively with the Cartesian co-ordinate of x, y and z.

3.1. Scour profile at the vicinity of the pier

The depth of the equilibrium scour profile at the vicinity of the pier was measured by a vernier point gauge with 5cm square grid range. The contour level is computed by subtracting the initial bed level and final scour bed level and the maximum scour depth is found to be 10.7 cm at front of the pier. From the contour is clearly visible that the scour hole resembles the inverted cone shape and the sediment deposition occurs at 30cm from the downstream of the pier.

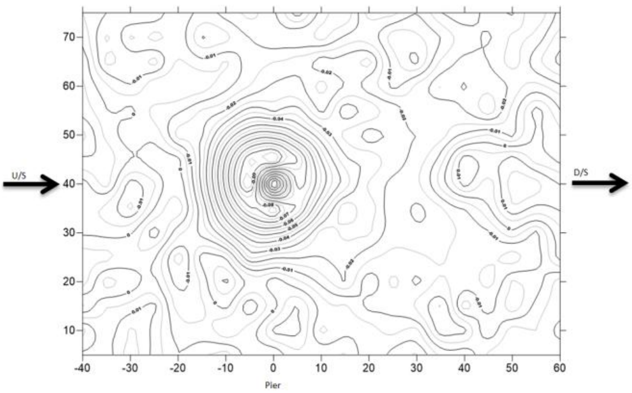

Fig.3. Contour of scour hole around cylindrical pier.

3.2. Velocity Distribution

In fig. 4 the time-averaged normalized longitudinal velocity u= u/U is shown vertically at different azimuthal planes at a vicinity of the pier. The flow at flatbed which outside the scour hole follows the law of wall up to 5 to 6 cm from the bed and at scour hole, the velocity is less but fluctuate in nature due to the formation of horseshoe vortex. Other than scour hole, the flow at flatbed follows a similar trend as found by [15].

At upstream of the pier, u velocity at scour hole is diminishing due to the stagnation pressure which occurred to the presence of pier. At the location of scour hole in the plane of symmetry the u velocity oscillates. At sides of the pier (90˚ and 270˚) there is no fluctuation at the base of the pier, which indicates the horseshoe vortex is diminished [3], the strength of the streamwise velocity is very minimum. From the graph, it is noticed that at downstream of the pier there is not much fluctuation found up to the boundary layer.

From the graph, it is found that from scour hole to up to 10 cm along the plane of symmetry at the downstream side of the pier is strongly affected by vortex shed. At downstream other than the plane of symmetry, flow at flatbed almost follows the similar trend except. The longitudinal velocity at the scour hole in downstream is highly oscillated due to the wake vortex.

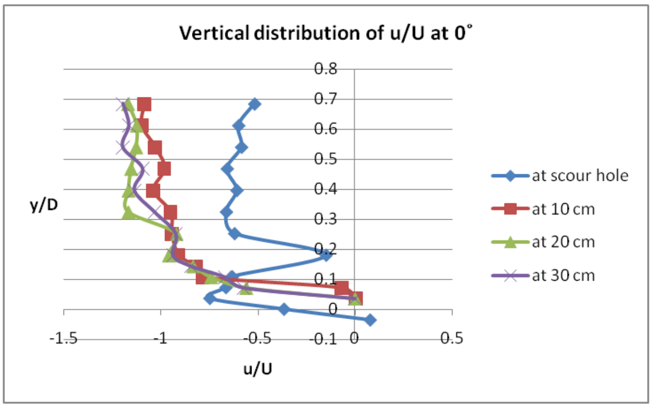

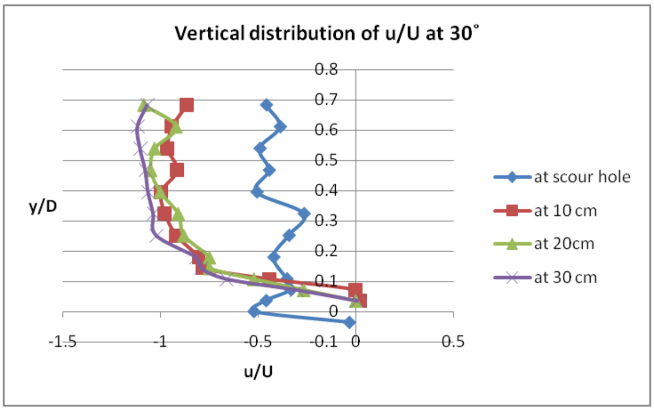

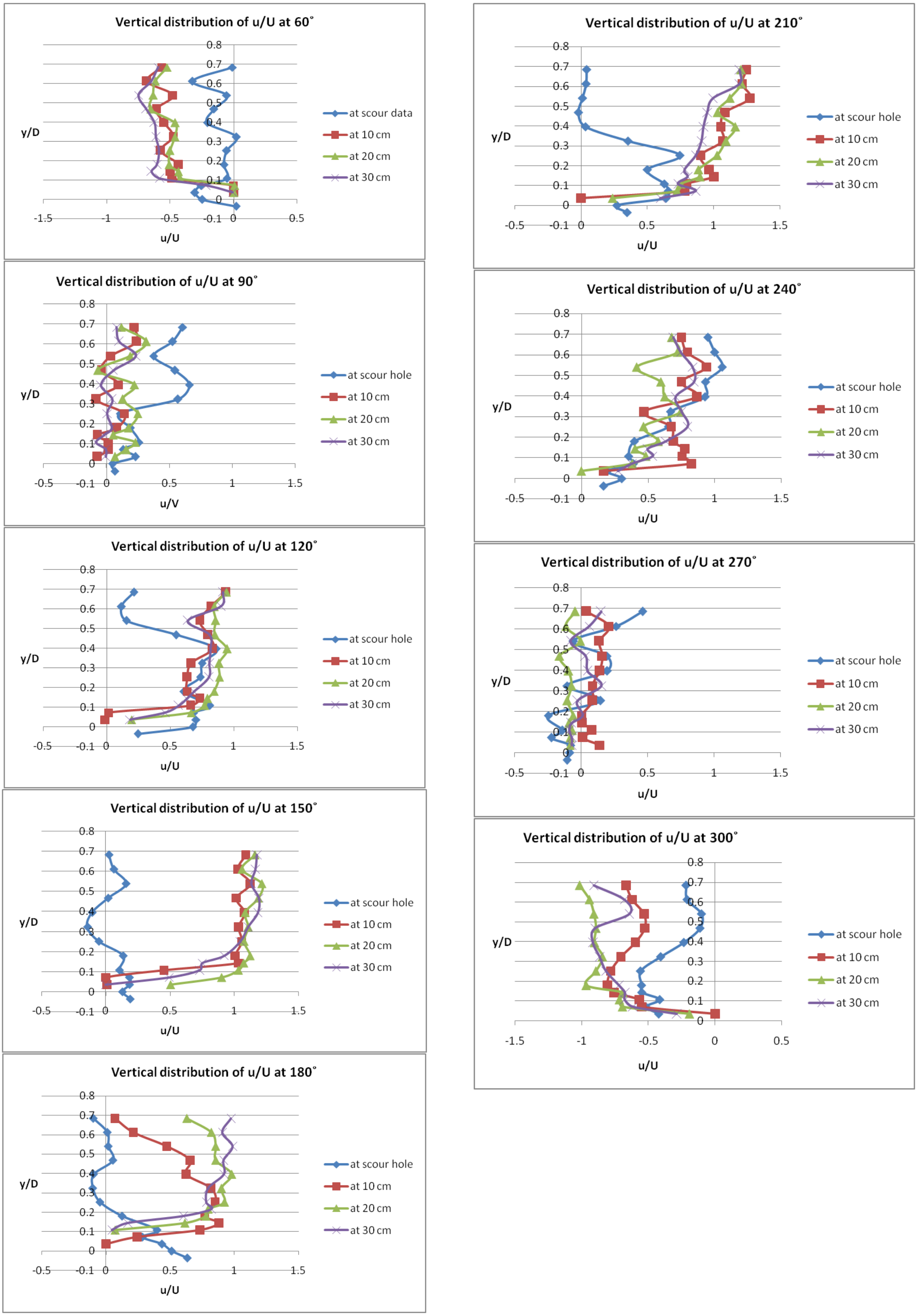

Fig.4. Vertical distribution of û at azimuthal sections: θ= 30˚, 60˚, 90˚, 120˚, 150˚, 180˚, 210˚, 240˚, 270˚, 300˚, 330˚ & 360˚.

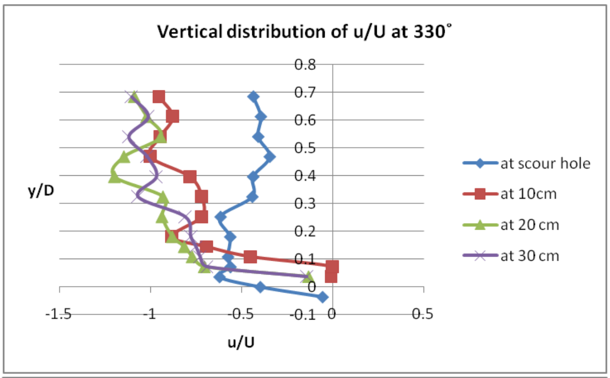

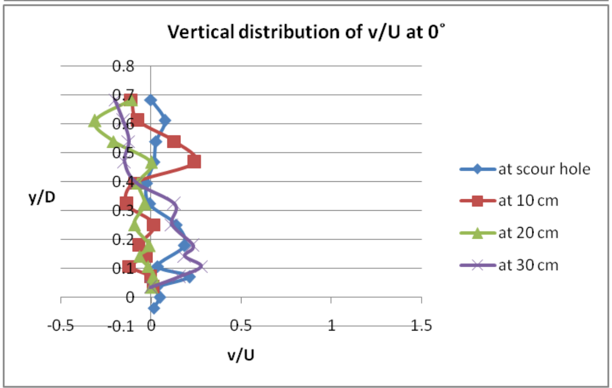

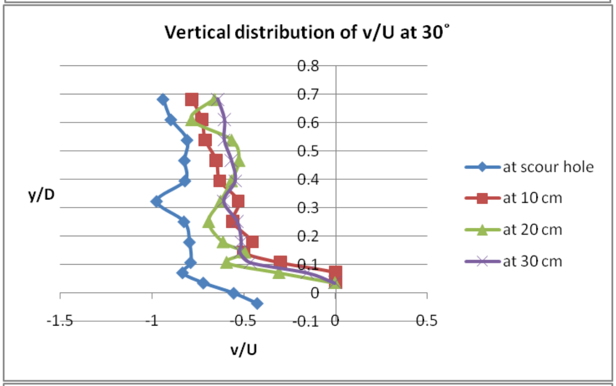

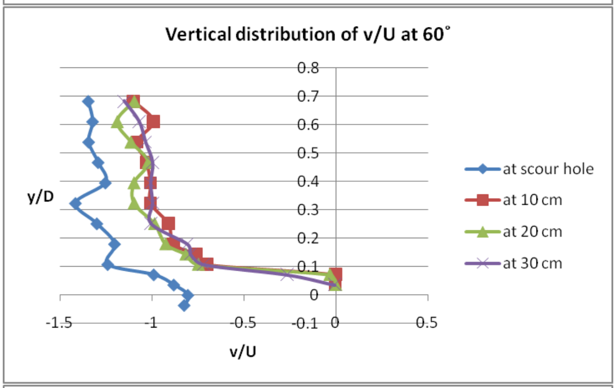

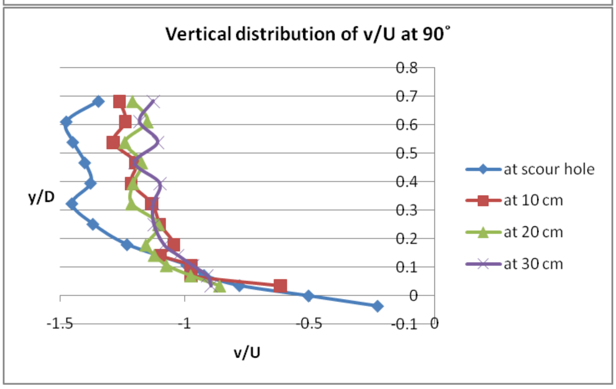

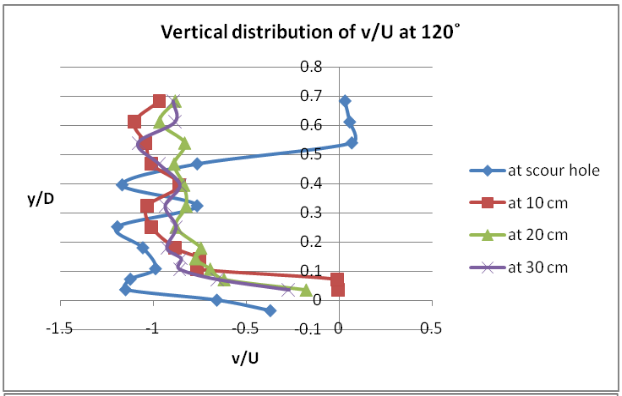

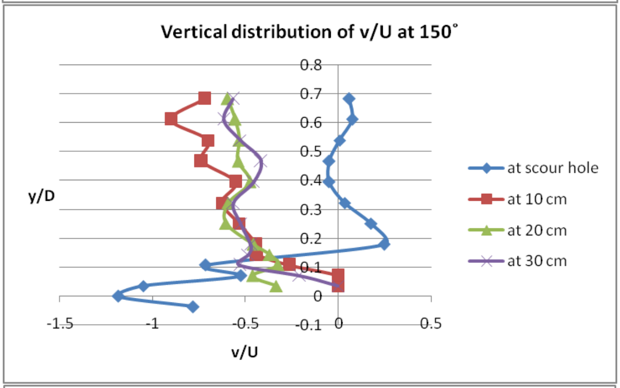

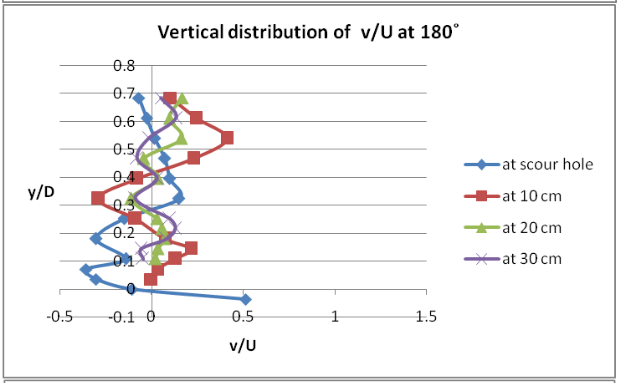

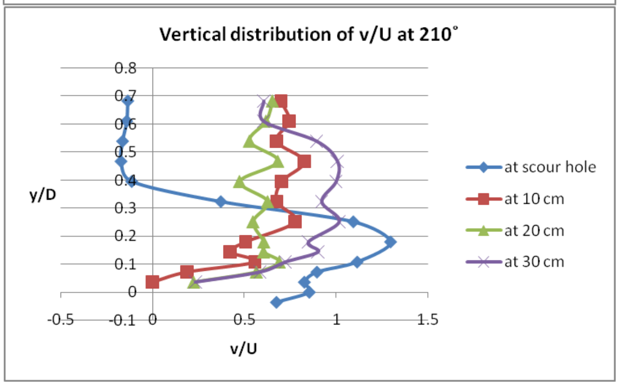

The normalized time averaged lateral velocity $\hat{v} = v/U$ at the vicinity of the pier of a different azimuthal plane is shown in fig.5. From the diagram, it is found that the variation in lateral velocity at upstream and sides of the pier follows the same trend except for the plane of symmetry. Both upstream and downstream plane of symmetry the magnitude is minimal, and it fluctuates due to periodical shedding at downstream.

At a downstream side of the pier (150˚ and 210˚) there, two primary vortices found among one is the clockwise vortex, and another one is anti-clockwise vortex as the same discovered by [10]. It is evident that the vortex at 150˚ is bigger than the vortex in 210˚, from the graph is visible the vortex started from 120˚.

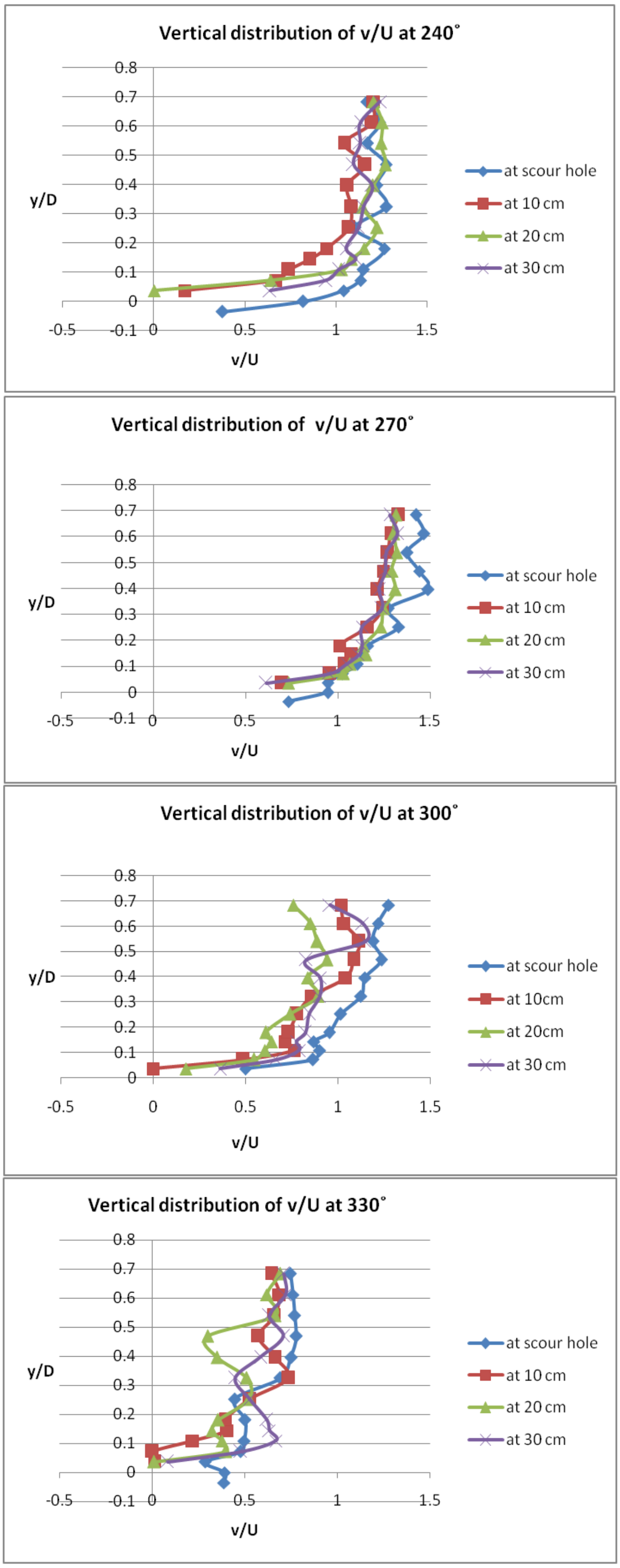

Fig.5. Vertical distribution of $\hat{v}$ at azimuthal sections: θ= 30˚, 60˚, 90˚, 120˚, 150˚, 180˚, 210˚, 240˚, 270˚, 300˚, 330˚ & 360˚.

The time-averaged normalized vertical velocity $\hat{w}$ = w/U is shown vertically at different planes around the pier in fig.6. The vertical velocity at upstream and sides of the pier is considerably retarded after the scour hole which is seen from the visual representation. Once the flow reached the scour hole the magnitude of vertical velocity getting stronger in the negative direction which indicates the downflow especially closer to the bed, the same was found by[7]. At downstream side in the plane of symmetry, vertical distribution of w velocity is formidable and oscillating entire flow depth due to the wake vortex.

3.3. Turbulent Intensity

Fig. 6 exhibits the time-averaged normalized turbulent intensity u+ = $(u'^2)^{0.5}$ /U, of streamwise direction and the standardized time-averaged turbulent intensity in lateral v+ [= $(v'^2)^{0.5}$ /U] and vertical w+ [= $(w'^2)^{0.5}$ /U] direction in figure 8 and 9 at different planes of cylindrical pier, where u′ is the fluctuation of u. The intensity of turbulent was calculated from the root mean square value of velocity fluctuations. The turbulent strength of tangential, radial and vertical direction shows a similar trend as it was found by [14].

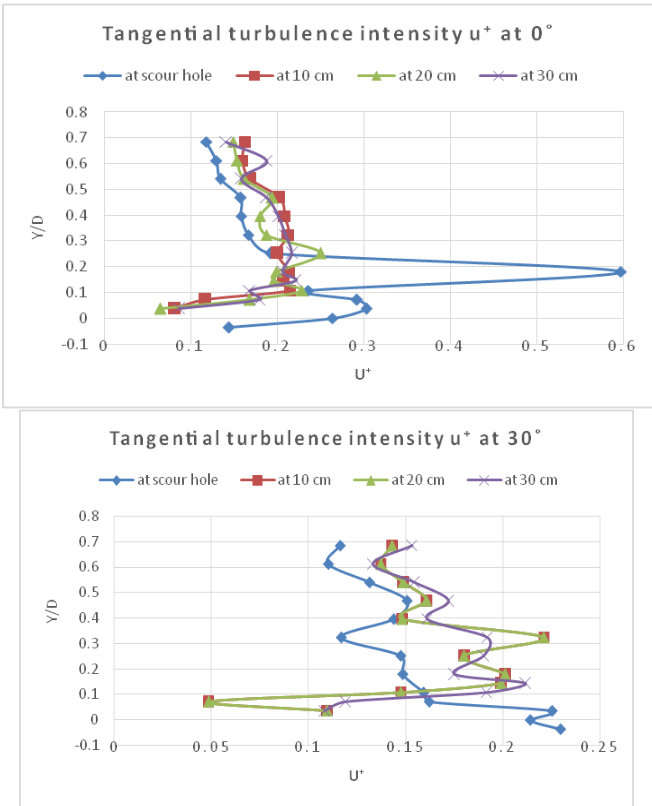

Published By:
Blue Eyes Intelligence Engineering
& Sciences Publication

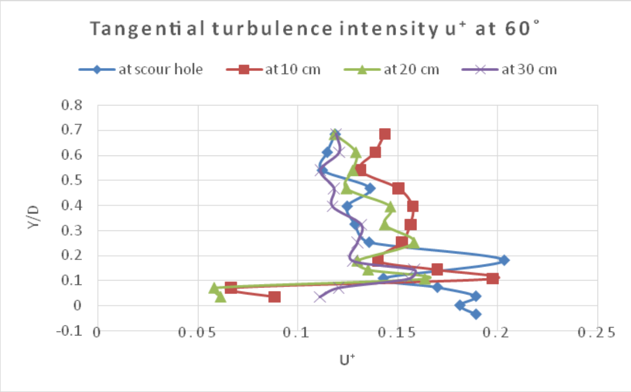
Tangential turbulence intensity u+ at 60°
at scour hole
at 10 cm
at 20 cm
at 30 cm
Y/D
U+

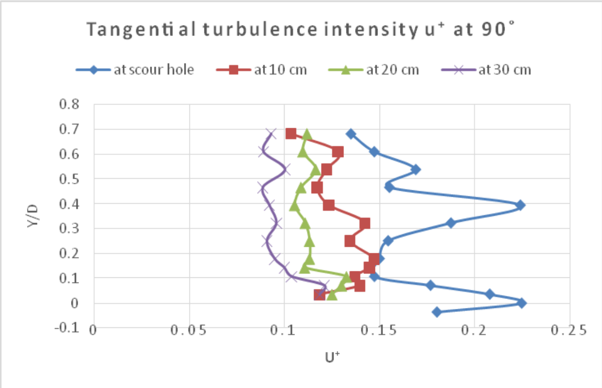
Tangential turbulence intensity u+ at 90°
at scour hole
at 10 cm
at 20 cm
at 30 cm
Y/D
U+

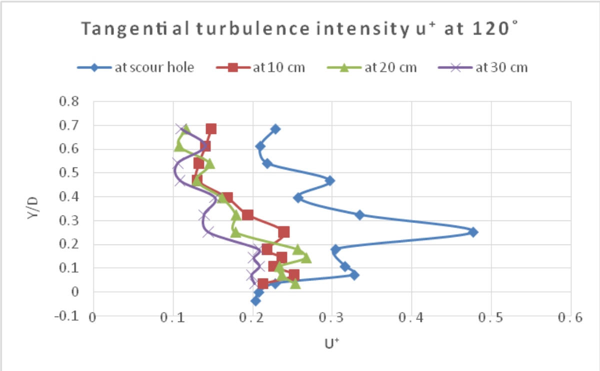
Tangential turbulence intensity u+ at 120°
at scour hole
at 10 cm
at 20 cm
at 30 cm
Y/D
U+

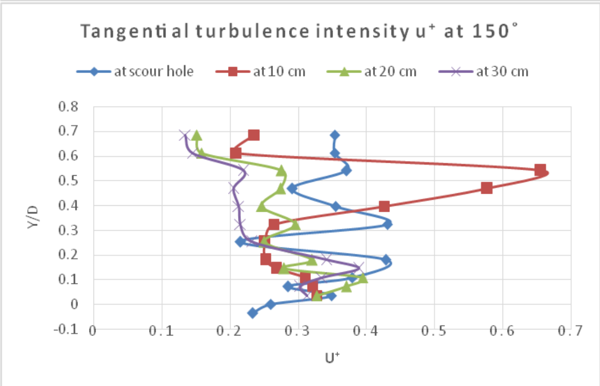
Tangential turbulence intensity u+ at 150°
at scour hole
at 10 cm
at 20 cm
at 30 cm
Y/D
U+

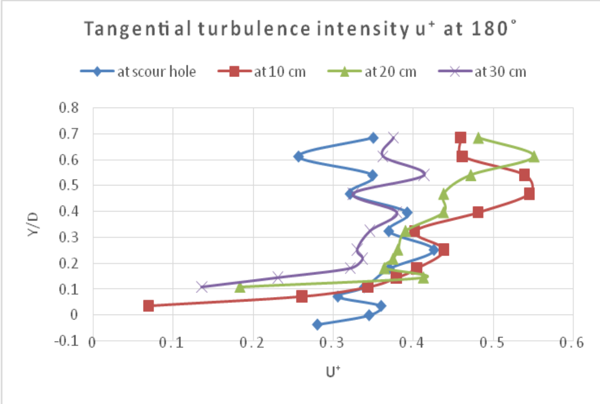
Tangential turbulence intensity u+ at 180°
at scour hole
at 10 cm
at 20 cm
at 30 cm
Y/D
U+

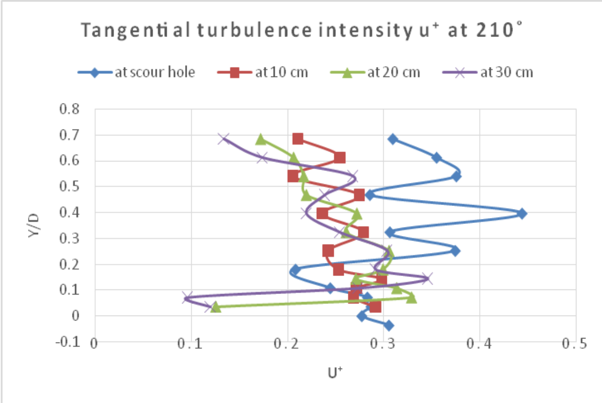
Tangential turbulence intensity u+ at 210°
at scour hole
at 10 cm
at 20 cm
at 30 cm
Y/D
U+

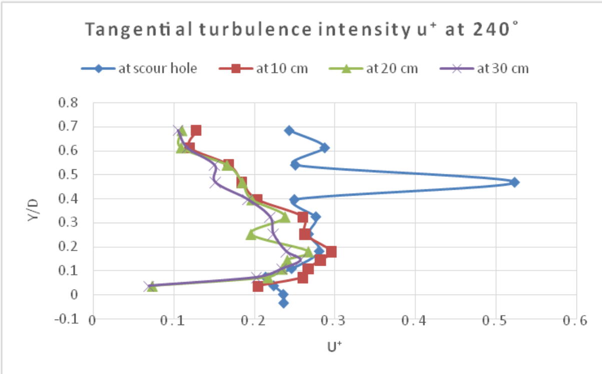
Tangential turbulence intensity u+ at 240°
at scour hole
at 10 cm
at 20 cm
at 30 cm
Y/D
U+

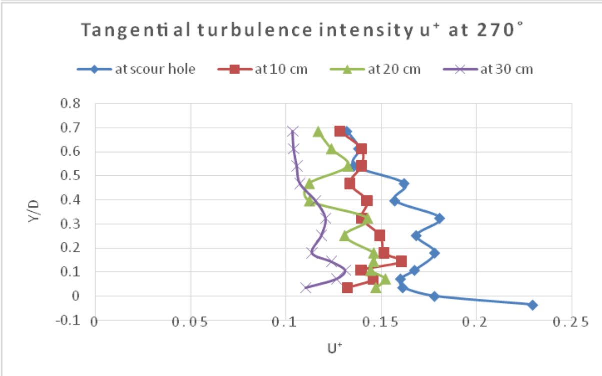
Tangential turbulence intensity u+ at 270°
at scour hole
at 10 cm
at 20 cm
at 30 cm
Y/D
U+

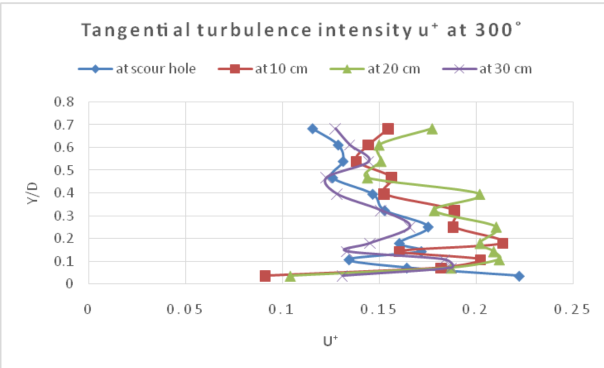
Tangential turbulence intensity u+ at 300°
at scour hole
at 10 cm
at 20 cm
at 30 cm
Y/D
U+

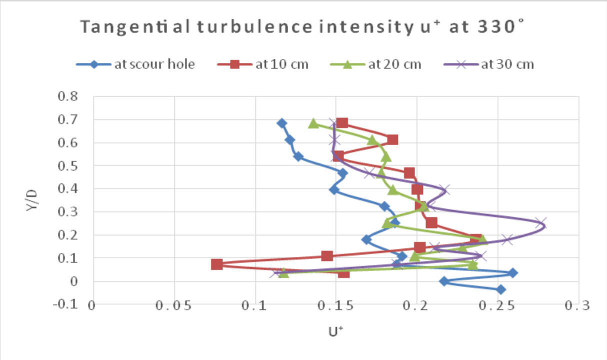

Fig.6. Vertical distribution of u⁺ at azimuthal sections: θ= 30˚, 60˚, 90˚, 120˚, 150˚, 180˚, 210˚, 240˚, 270˚, 300˚, 330˚ & 360˚.

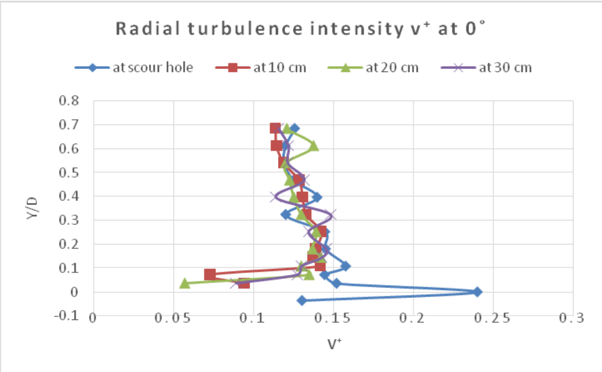

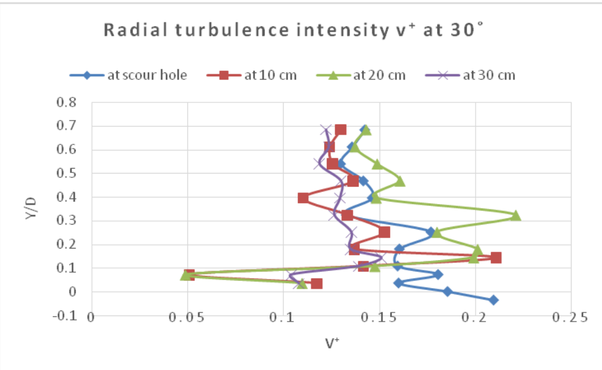

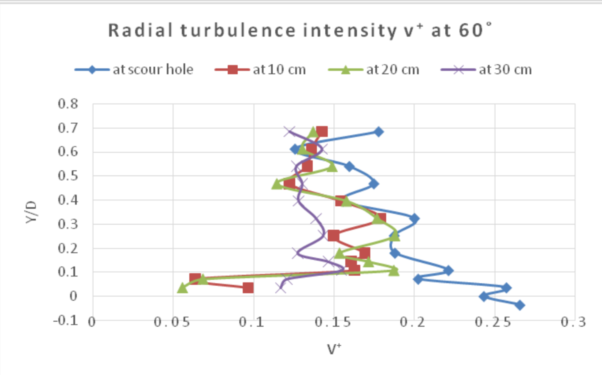

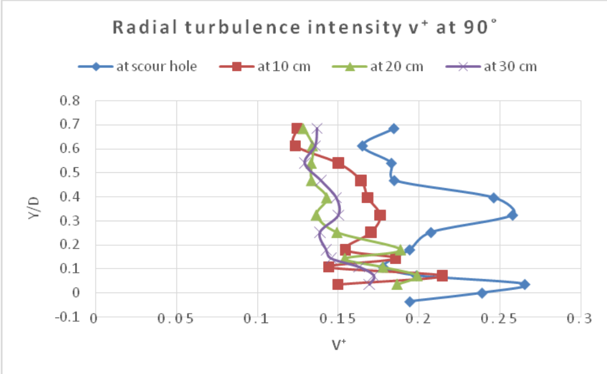

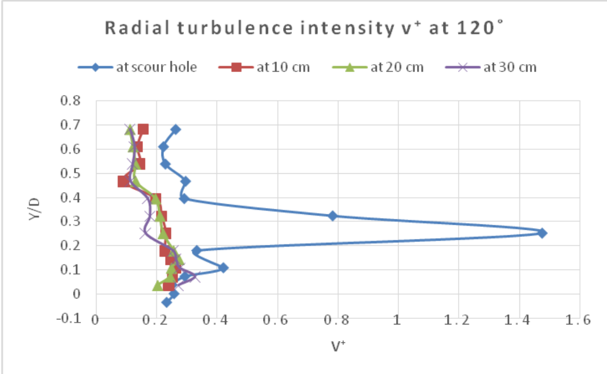

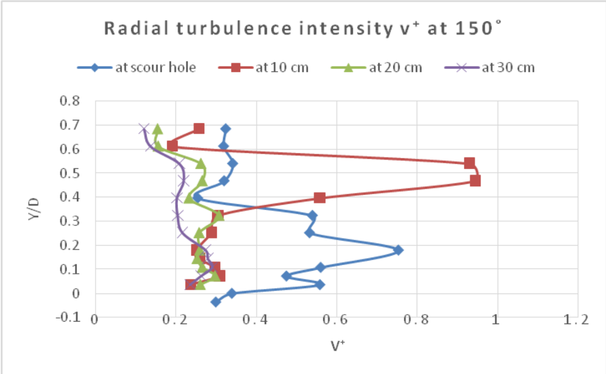

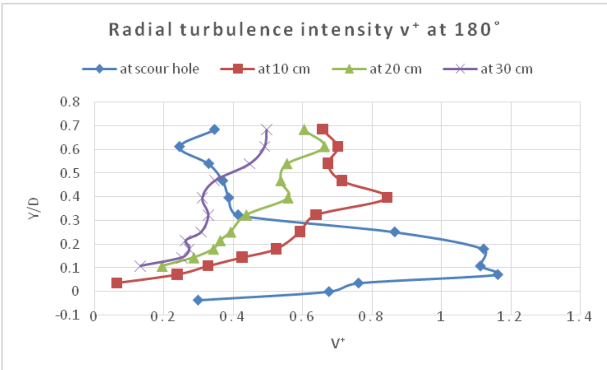

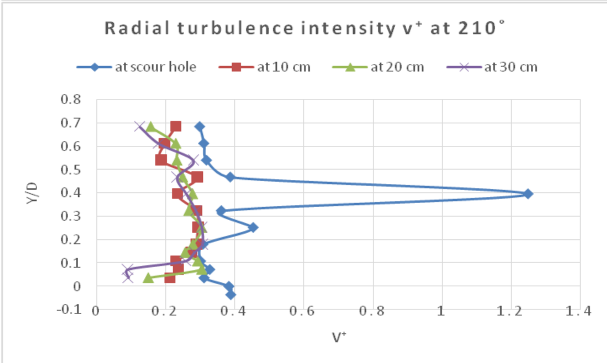

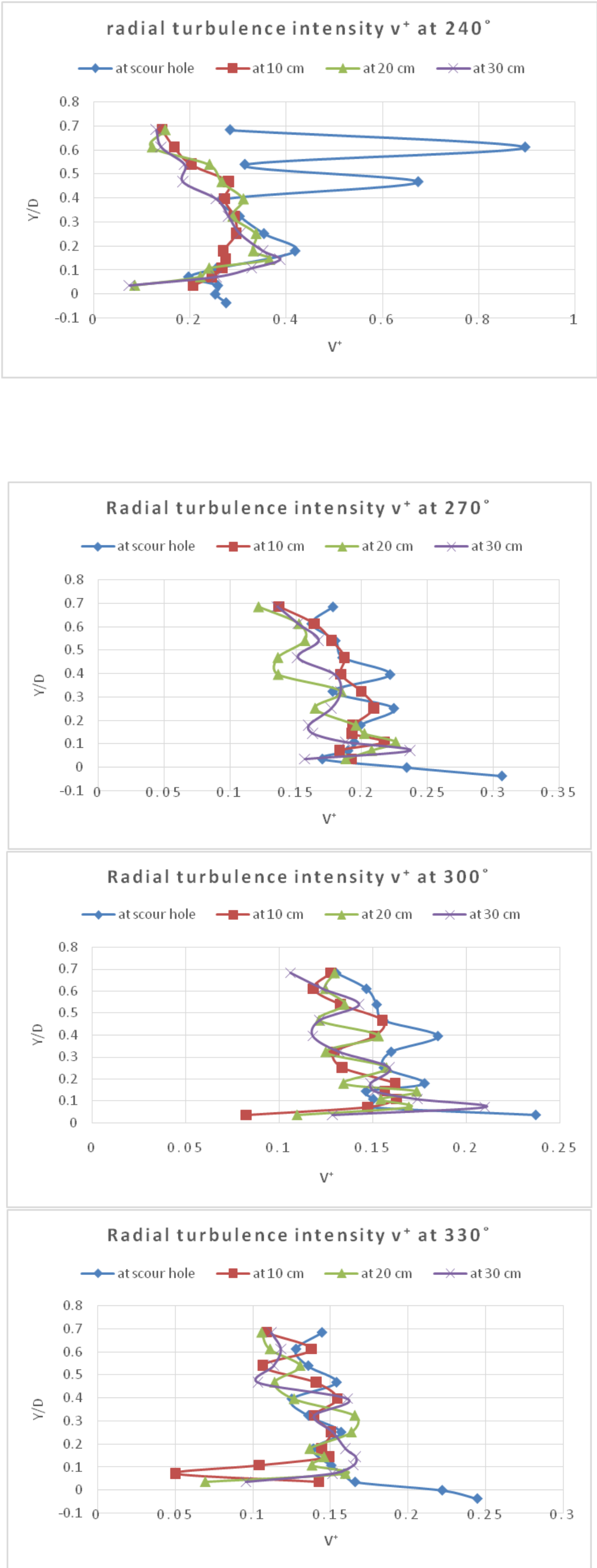

Fig.7. Vertical distribution of v^+ at azimuthal sections: θ= 30˚, 60˚, 90˚, 120˚, 150˚, 180˚, 210˚, 240˚, 270˚, 300˚, 330˚ & 360˚.

From chart 6, it is evident that the turbulent intensity in the upstream side, on the plane of symmetry is high as seen by [3]. At the upstream side of the pier, both the flanks from plane of symmetry the magnitude of turbulent intensity is getting retarded as the angles as well as lateral distance is increased. And it is reached the minimal values at sides of the pier as the same was found by[14]. The turbulent intensity is strong in downstream of the pier than upstream as it was said by[7].

The radial turbulent intensity is minimum at the upstream side and maximum at a downstream side of the pier. At downstream side, compared to the plane of symmetry the magnitude of turbulence at scour hole is high at 120˚ and 210˚. This observation shows that the powerful vortices formed both the sides of the plane of symmetry and the magnitude is maximum in 120˚ than others.

The vertical turbulent intensity plot is not shown here due to space restrain, moreover the magnitude of vertical turbulence is minimum and negligible. In an upstream side of the pier the strength of turbulent at scour hole have pronounced bulges at the near bed, and the turbulent intensity at 10, 20 and 30 cm follows the similar trend. At downstream side the magnitude is high when compared to upstream side and it reaches the maximum value at the plane of symmetry, it is fluctuating in nature.

3.4. Turbulent Kinetic Energy

In fig.8 depicts the vertical distribution of time-averaged normalized kinetic energy at vicinity of pier $\hat{K}$ = [k/U2 =0.5(u$^+$2+ v$^+$2 + w$^+$2)]. The core of turbulent kinetic energy is found in the rear side of the pier due to the frequent shedding of the vortex which is seen from the illustration. In the upstream side, the magnitude of K is comparatively less as it was found by[16].

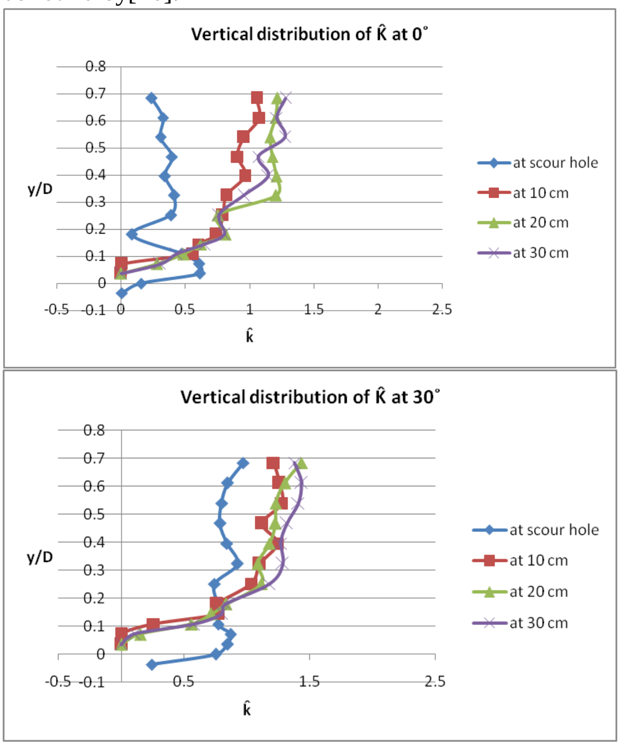

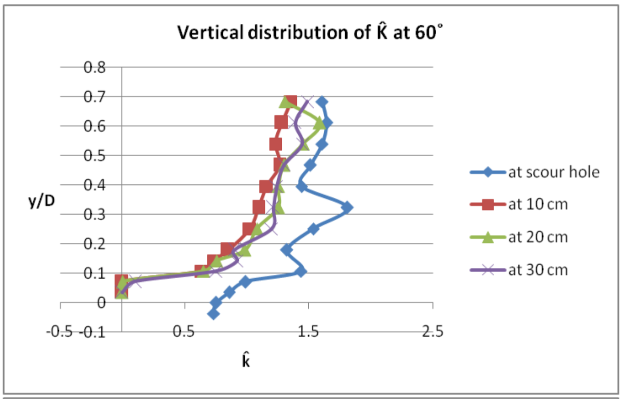
Vertical distribution of K̂ at 60°
y/D
K̂
at scour hole
at 10 cm
at 20 cm
at 30 cm

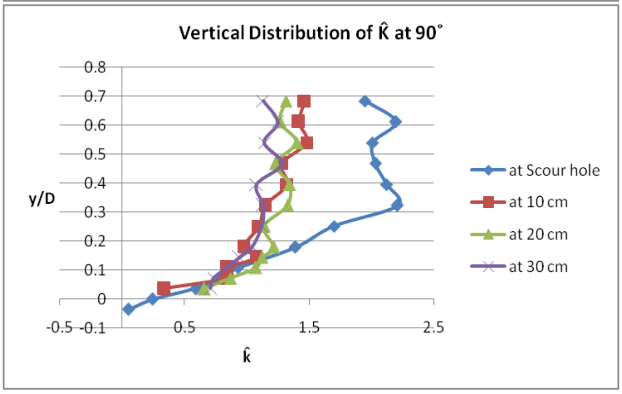
Vertical Distribution of K̂ at 90°
y/D
K̂
at Scour hole
at 10 cm
at 20 cm
at 30 cm

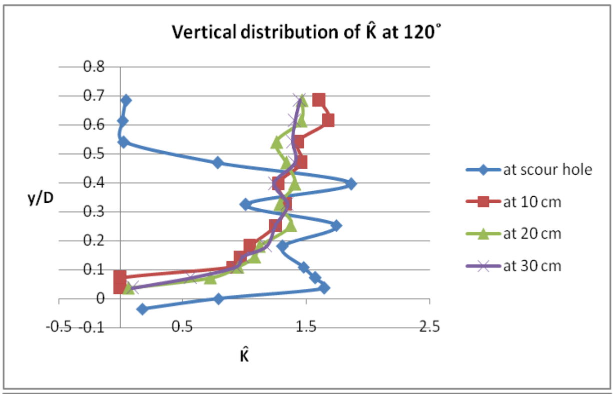
Vertical distribution of K̂ at 120°
y/D
K̂
at scour hole
at 10 cm
at 20 cm
at 30 cm

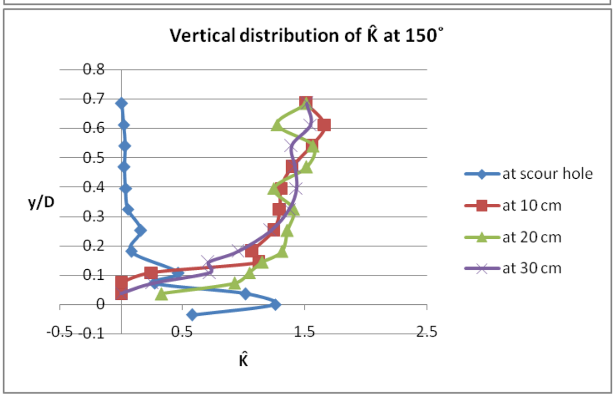
Vertical distribution of K̂ at 150°
y/D
K̂
at scour hole
at 10 cm
at 20 cm
at 30 cm

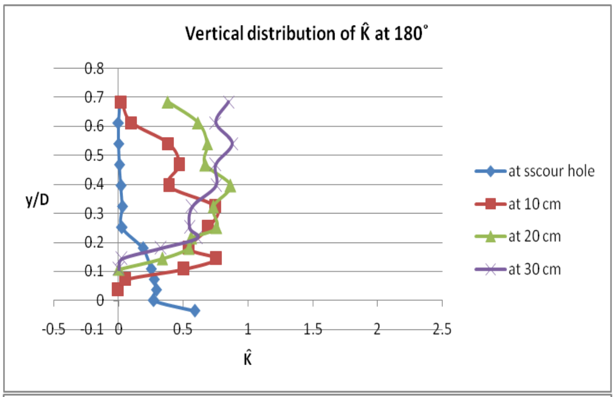
Vertical distribution of K̂ at 180°
y/D
K̂
at sscour hole
at 10 cm
at 20 cm
at 30 cm

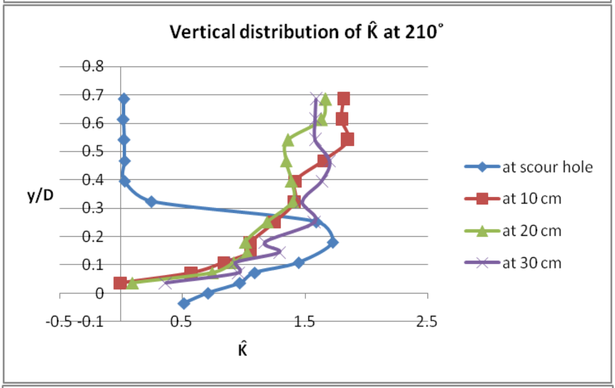
Vertical distribution of K̂ at 210°
y/D
K̂
at scour hole
at 10 cm
at 20 cm
at 30 cm

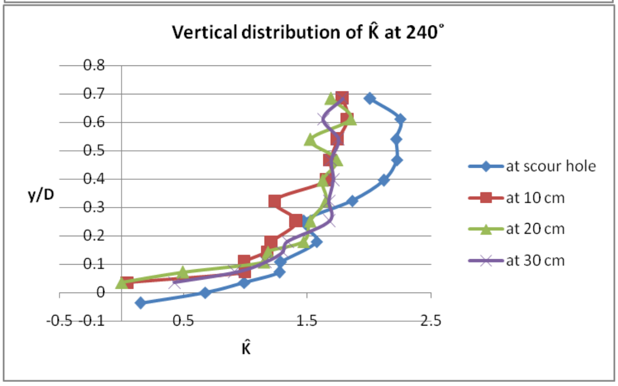
Vertical distribution of K̂ at 240°
y/D
K̂
at scour hole
at 10 cm
at 20 cm
at 30 cm

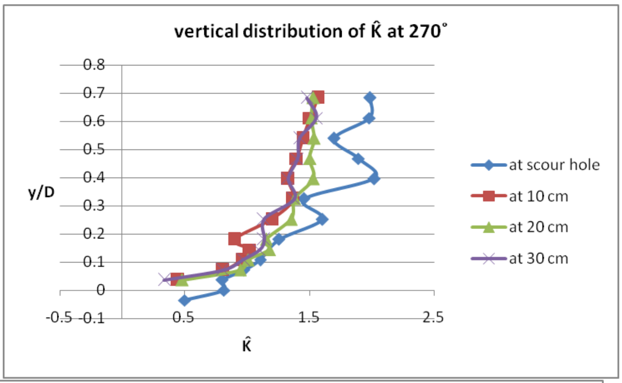
vertical distribution of K̂ at 270°
y/D
K̂
at scour hole
at 10 cm
at 20 cm
at 30 cm

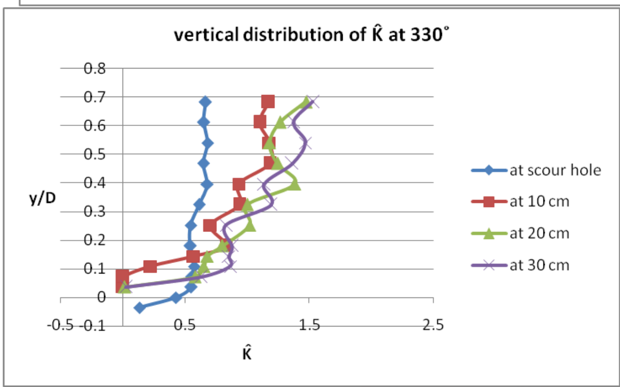
vertical distribution of K̂ at 330°
y/D
K̂
at scour hole
at 10 cm
at 20 cm
at 30 cm

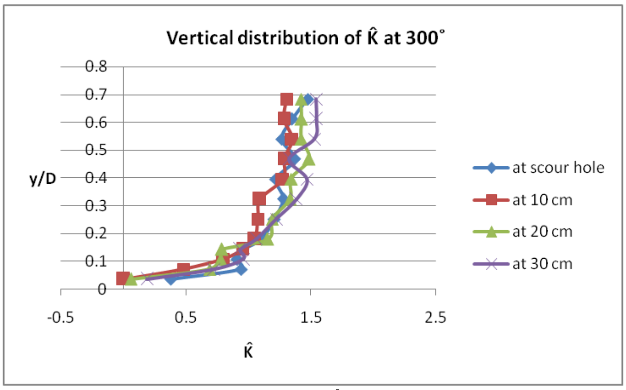

Fig.8. Vertical distribution of K̂ at azimuthal sections: θ= 30˚, 60˚, 90˚, 120˚, 150˚, 180˚, 210˚, 240˚, 270˚, 300˚, 330˚ & 360˚.

Inside the scour hole the magnitude of K̂ at plane of symmetry is minimum when compared to other places. The magnitude of K̂ is high at sides of the pier and very minimum at a downstream side at the plane of symmetry where the separation of flow occurs due to the formation of two paramount vortices. At downstream side, from 120 degree to 210 degree the magnitude of kinetic energy at inside the scour hole is bulges near bed surface and above that the magnitude is very minimum.

3.5. Reynolds Stress

The normalized Reynolds stress of tangential direction uw^+ $[= -u'w'/u_*^2]$, radial direction vw^+ $[= -v'w'/u_*^2]$ and at different section around the pier are plotted, Where u'= velocity fluctuation of u, v'= velocity fluctuation of v, w'= velocity fluctuation of w and u_* = shear velocity of approaching flow.

The figure 9 depicts that the Reynolds stress at upstream is reasonably linear from the plane of symmetry as the same found by [7] and at plane of symmetry of upstream and downstream it reaches the maximum values and retarded in nature towards the sides of the pier. In the upstream side, a notable bulge of uw^+ occurs in scour hole just above the bed level.

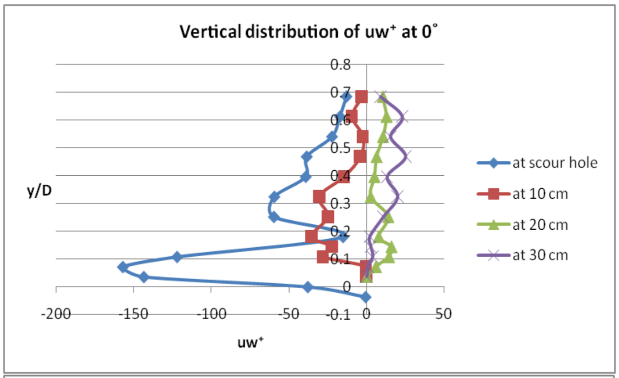

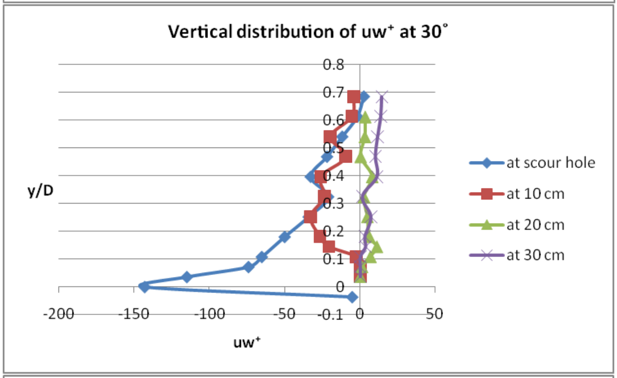

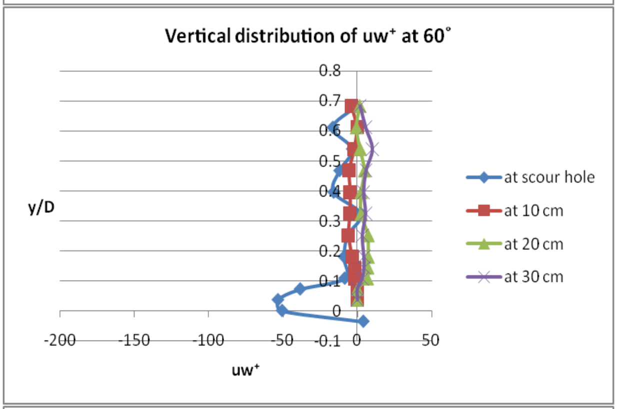

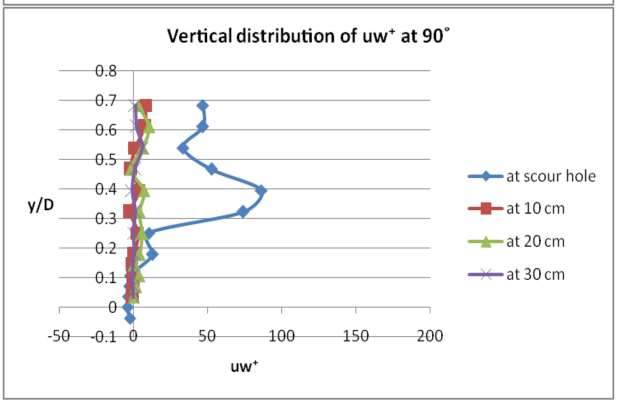

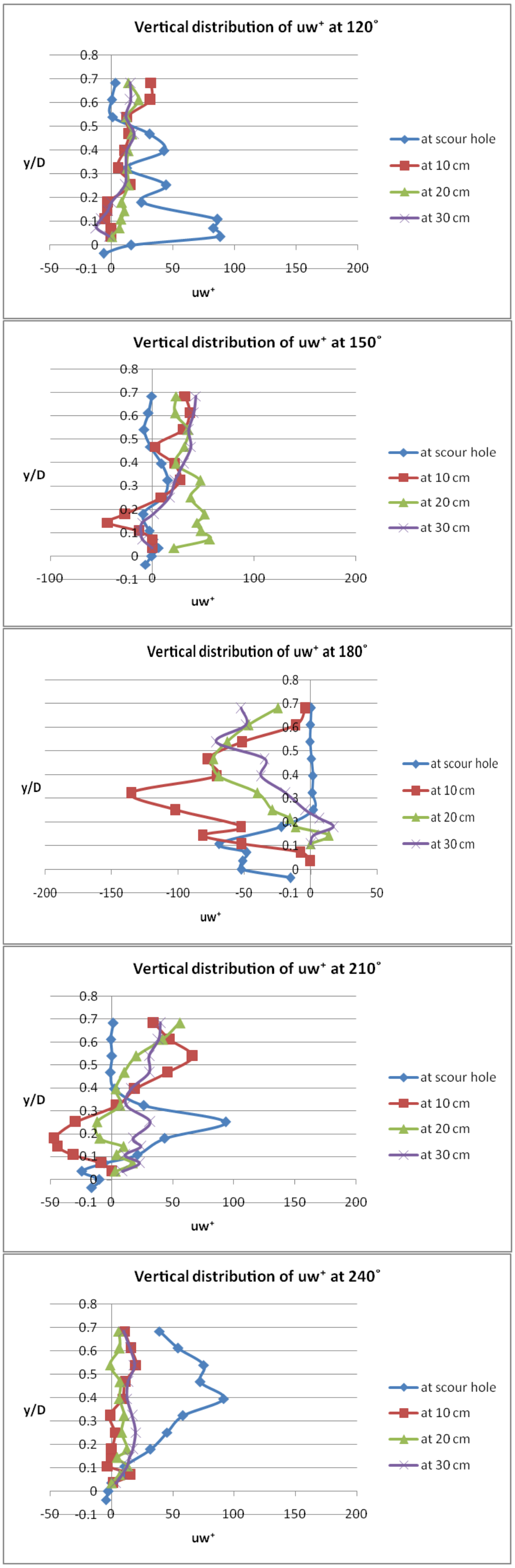

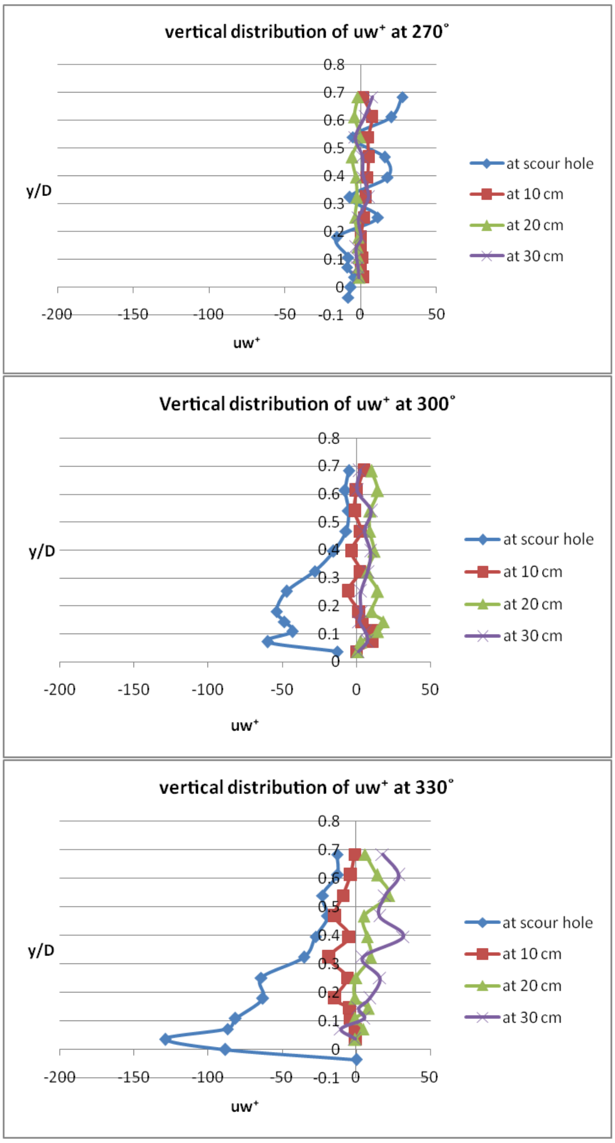

Fig.9. Vertical distribution of uw⁺ at azimuthal sections: θ= 30˚, 60˚, 90˚, 120˚, 150˚, 180˚, 210˚, 240˚, 270˚, 300˚, 330˚ & 360˚.

The magnitude of uv^+ is high in the wake region of the pier when compared to uw^+ and vw^+ as the same found by [17]. In contrary to uw^+ in a plane of symmetry, the values of uv^+ and vw^+ are minimum. In 120˚ and 240˚, the values of uv^+ are high due to the formation of two Primary vortexes and magnitude is high at 240˚ than 120˚.

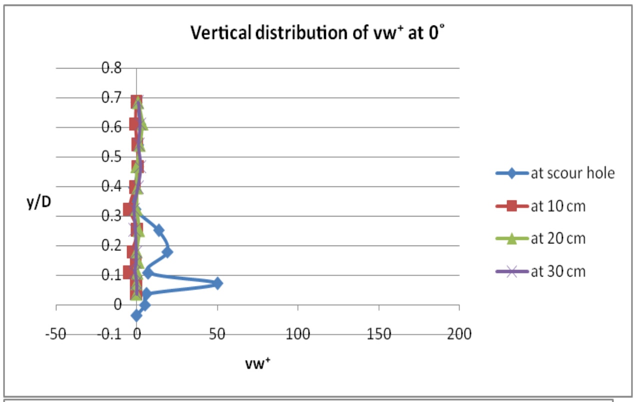

Vertical distribution of vw⁺ at 0˚

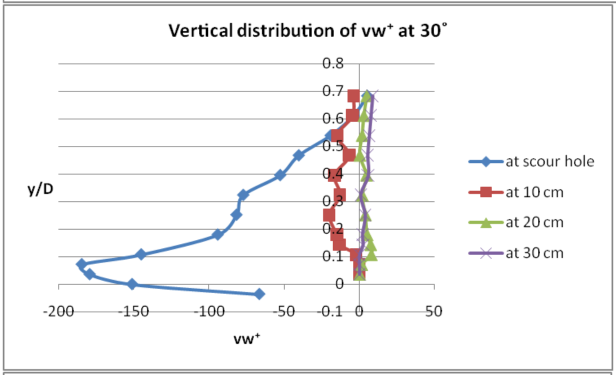

Vertical distribution of vw⁺ at 30˚

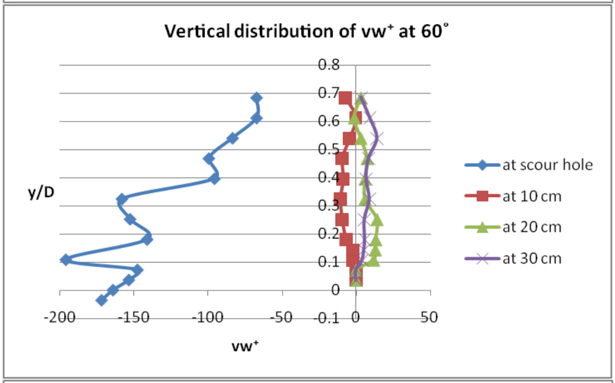

Vertical distribution of vw⁺ at 60˚

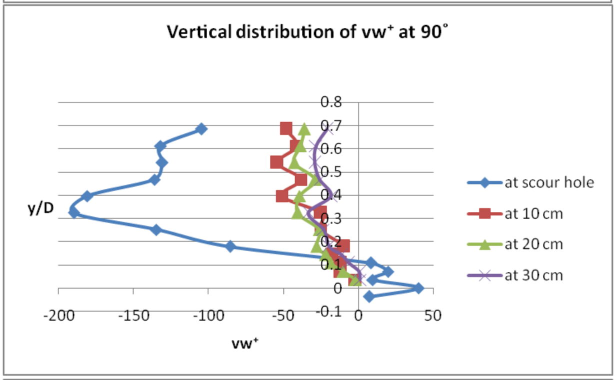

Vertical distribution of vw⁺ at 90˚

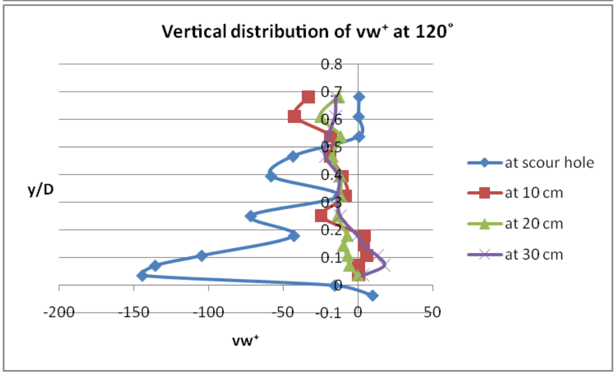

Vertical distribution of vw⁺ at 120˚

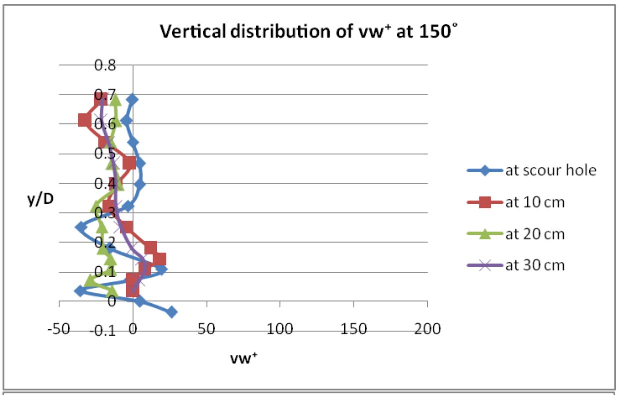

Vertical distribution of vw⁺ at 150˚

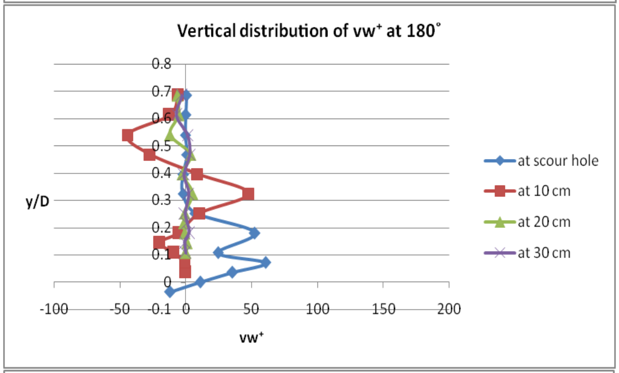

Vertical distribution of vw⁺ at 180˚

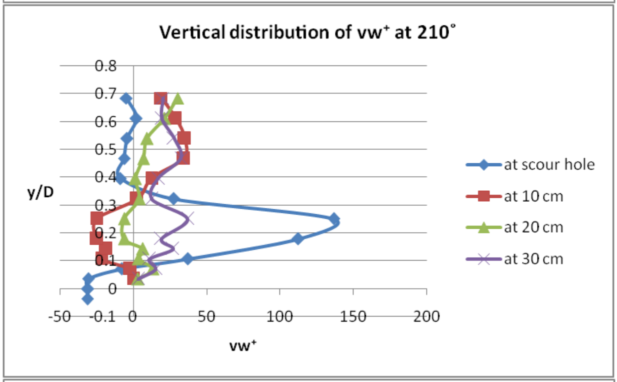

Vertical distribution of vw⁺ at 210˚

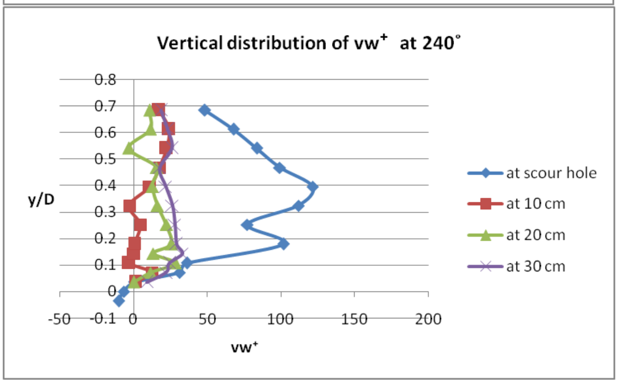

Vertical distribution of vw⁺ at 240˚

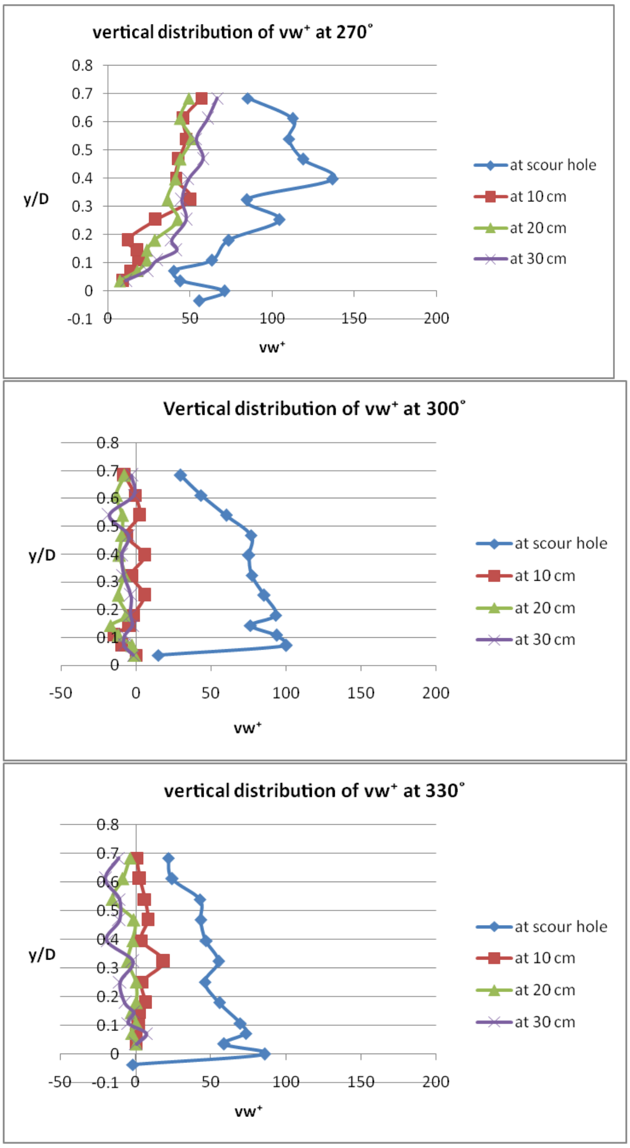

Fig.10. Vertical distribution of uv⁺ at azimuthal sections: θ= 30˚, 60˚, 90˚, 120˚, 150˚, 180˚, 210˚, 240˚, 270˚, 300˚, 330˚ & 360˚.

The value of vw⁺ at sides of the pier is high and retarded towards the plane of symmetry and attains the minimum values. The graph of vw⁺ not shown here, because not showing any unique trend, moreover the Magnitude of vw⁺ in 10, 20 and 30 cm around the pier is very minimum and negligible except at scour hole.

IV. CONCLUSION

The velocity and turbulent flow around cylindrical pier with the scour hole under clear water condition was measured with ADV. The normalized plots of velocity, turbulent intensity, Reynolds shear stress at different azimuthal section of pier has shown in this study which can provide the better understanding of the flow behaviour at inside and outside the scour hole.

- Before The flow near bed at outside the scour hole follows the law of wall up to 6 cm. At sides of the pier, there is no fluctuation at the base of the pier, which indicates the horseshoe vortex is diminished; the strength of the stream-wise velocity is very minimum.
- The lateral velocity shows two primary vortexes formed at wake region of pier and one is clockwise and another oneanti-clock wise in nature with asymmetrical magnitude.
- The turbulent intensityat tangential direction is high in the plane of symmetry and it gets diminishes when the angle and lateral distances increases.
- The magnitude of kinetic energy is high at sides of the pier and low at the line of symmetry.

Taking velocity data at inside the scour hole is very difficult due to shape of scour hole as it is resembles the inverted cone where one of the ADV receiver touch the bed and other two receiver is little away from the bed, further study need to be conducted to overcome this issue.

V. REFERENCES

1. M. Zhao, L. Cheng, and Z. Zang, "Experimental and numerical investigation of local scour around a submerged vertical circular cylinder in steady currents". *Coastal Engineering*. 2010. 57(8). Pp. 709–721. DOI:10.1016/j.coastaleng.2010.03.002. URL: http://dx.doi.org/10.1016/j.coastaleng.2010.03.002
2. D. Bijan, "Controlling Mechanism of Local Scouring". *Journal of Hydraulic Engineering*. 1990. 116(10). Pp. 1197–1214. DOI:10.1061/(ASCE)0733-9429(1990)116:10(1197). URL: https://doi.org/10.1061/(ASCE)0733-9429(1990)116:10(1197)
3. S. Dey and R.V. Raikar, "Characteristics of Horseshoe Vortex in Developing Scour Holes at Piers". *Journal of Hydraulic Engineering*. 2007. 133(4). Pp. 399–413. DOI:10.1061/(asce)0733-9429(2007)133:4(399)
4. A. Kumar, and U.C. Kothyari, "Three-Dimensional Flow Characteristics within the Scour Hole around Circular Uniform and Compound Piers". *Journal of hydraulic engineering*, 2012. DOI:10.1061/(ASCE)HY.1943-7900.
5. B.W. Melville, Local scour at bridge sites. 1975.
6. B.W. Melville, and A.J. Raudkivi, "Flow Characteristics in Local Scour At Bridge Piers". *Journal of Hydraulic Research*. 2010. 15(4). Pp. 373–380. DOI:10.1080/00221687709499641.
7. W.H. Graf, and I. Istiarto, "Flow pattern in the scour hole around a cylinder Flow pattern in the scour hole around a cylinder." *Journal of Hydraulic Research*. 2002. 40(1). Pp. 22–1686. DOI:10.1080/00221680209499869
8. F. Ahmed, and N. Rajaratnam, "Flow around Bridge Piers". *Journal of Hydraulic Engineering*. 2002. 124(3). Pp. 288–300. DOI:10.1061/(asce)0733-9429(1998)124:3(288).
9. H.N.C. Breusers, G. Nicollet, and H.W. Shen. "Local Scour Around Cylindrical Piers". *Journal of Hydraulic Research*. 2010. 15(3). Pp. 211–252. DOI:10.1080/00221687709499645.
10. R. Ettema, G. Kirkil, and M. Muste. "Similitude of Large-Scale Turbulence in Experiments on Local Scour at Cylinders". *Journal of Hydraulic Engineering*. 2005. 132(1). Pp. 33–40. DOI:10.1061/(asce)0733-9429(2006)132:1(33).
11. B. Dargahi. "The turbulent flow field around a circular cylinder". *Experiments in Fluids*. 1989. 8(1–2). Pp. 1–12. DOI:10.1007/BF00203058.
12. F. Ahmed, and N. Rajaratnam. "The three-dimensional turbulent boundary layer flow around bridge piers". *Journal of Hydraulic Research*. 1997. 35(2). Pp. 209–224. DOI:10.1080/00221689709498427
13. K. Debnath, M.K. Manik, and B.S. Mazumder. "Turbulence statistics of flow over scoured cohesive sediment bed around circular cylinder". *Advances in Water Resources*. 2012. 41. Pp. 18–28. DOI:10.1016/j.advwatres.2012.02.008. URL: http://dx.doi.org/10.1016/j.advwatres.2012.02.008.
14. S. Das and A. Mazumdar. "Turbulence flow field around two eccentric circular piers in scour hole". *International Journal of River Basin Management*. 2015. 13(3). Pp. 343–361. DOI:10.1080/15715124.2015.1012515.
15. A. Kumar, U.C, Kothyari, and K.G. Ranga Raju. "Flow structure and scour around circular compound bridge piers - A review". *Journal of Hydro-Environment Research*. 2012. 6(4). Pp. 251–265. DOI:10.1016/j.jher.2012.05.00 6. URL:

http://dx.doi.org/10.1016/j.jher.2012.05.006.

16. B. Ataie-Ashtiani and A. Aslani-Kordkandi. "Flow field around side-by-side piers with and without a scour hole. European Journal of Mechanics, B/Fluids. 2012. 36. Pp. 152–166. DOI:10.1016/j.euromechflu.2012.03.007.
17. B. Ataie-Ashtiani and A. Aslani-Kordkandi. "Flow field around single and tandem piers". *Flow, Turbulence and Combustion*. 2013. 90(3). Pp. 471–490. DOI:10.1007/s10494-012-9427-7.
18. J.E. Richardson and V.G. Panchang. "Three-Dimensional Simulation of Scour-Inducing Flow at Bridge Piers". *Journal of Hydraulic Engineering.* 2002. 124(5). Pp. 530–540. DOI:10.1061/(asce)0733-9429(1998)124:5(530).
19. G. Kirkil, G. Constantinescu and R. Ettema. "The Horseshoe Vortex System Around a Circular Bridge Pier on Equilibrium Scoured Bed". *In Impacts of global climate change,* 2005. Pp. 1–12. DOI:10.1061/40792(173)414.
20. T.M. Salaheldin, J. Imran and M.H. Chaudhry. "Numerical Modeling of Three-Dimensional Flow Field Around Circular Piers". *Journal of Hydraulic Engineering*. 2004. 130(2). Pp. 91–100. DOI:10.1061/(asce)0733-9429(2004)130:2(91).
21. W. Huang, Q. Yang and H. Xiao. "CFD modeling of scale effects on turbulence flow and scour around bridge piers". *Computers and Fluids*. 2009. 38(5). Pp. 1050–1058. DOI:10.1016/j.compfluid.2008.01.029. URL: http://dx.doi.org/10.1016/j.compfluid.2008.01.029.
22. U.C. Kothyari and A. Kumar. "Temporal Variation of Scour around Circular Compound Piers". *Journal of Hydraulic Engineering.* 2012. 138(11). Pp. 945–957. DOI:10.1061/(asce)hy.1943-7900.0000593.
23. Y. Chiew. "Scour Protection at Bridge Piers". *Journal of Hydraulic Engineering*. 2007. 118(9). Pp. 1260–1269. DOI:10.1061/(asce)0733-9429(1992)118:9(1260).
24. B.W. Melville and Y.M. Chiew. "TIME SCALE FOR LOCAL SCOUR AT BRIDGE PIERS", 1999.
25. D.G. Goring and V.I. Nikora. "Despiking Acoustic Doppler Velocimeter Data". *Journal of Hydraulic Engineering*. 2002. 128(1). Pp. 117–126. DOI:10.1061/(asce)0733-9429(2002)128:1(117).
26. V.I. Nikora. Discussions and Closures 133. 2003. 128(1). Pp. 2009.
27. F. Bhuiyan, R.D. Hey and P.R. Wormleaton. "Hydraulic Evaluation of W-Weir for River Restoration". *Journal of Hydraulic Engineering*. 2007. 133(6). Pp. 596–609. DOI:10.1061/(asce)0733-9429(2007)133:6(596).
28. A.K. Barbhuiya and S. Dey. "Measurement of turbulent flow field at a vertical semicircular cylinder attached to the sidewall of a rectangular channel". *Flow Measurement and Instrumentation*. 2004. 15(2). Pp. 87–96. DOI:10.1016/j.flowmeasinst.2003.11.002.

AUTHORS PROFILE

Mr. R. Karthik, completed his M.Tech in Water resources Engineering at NIT Silchar and working as a research scholar at same institute. He has published 4 research articles. Karthik is an associate member of IEI. His area of interest is experimental and computational analysis of Local Scour and its countermeasures at hydraulics structures.

Prof. Upendra Kumar, completed his Bachelor's Degree in Civil Engineering from Bhagalpur College of Engineering in 1994 and his Master of Civil Engineering with specialization in Environmental Engineering, from Jadavpur University, Kolkata, India in 1997 and Ph. D. in Civil Engineering with specialization in Environmental Engineering, from Indian Institute of Technology, Kharagpur, India in 2005. At present he is holding the post of Professor in the Department of Civil Engineering at National Institute of Technology, Silchar. He has published 66 number of Research Paper in total out of which 26 are in reputed Journals, 04 in edited books and the rest in Conferences. He has more than 600 Citation in International Journals. Current and previous research interests area includes Environmental Engineering; Water and Wastewater Engineering; Air and Noise Pollution; Adsorption technology.

Dr. Kumar is also the Fellow Member of International Congress of Environmental Research (F.I.C.E.R.), Senior Member of IACSIT, Senior Member of Asia-Pacific Chemical, Biological& Environmental Engineering Society (APCBEES) and Life Member of Institution of Engineers (India). Dr. Kumar is also associated with some Important International Journals as Referee and Reviewer.

Prof. Abdul Karim Barbhuiya is currently holding the post of Professor, Civil Engineering Department, National Institute of Technology, Silchar. He joined this Institute in the year 1994 as lecturer and thereafter completed his Ph.D. from IIT Kharagpur in 2003. His area of interest includes Local scour around obstructions, Riverbank erosion, Sediment transport, Watershed management. He has published more than 20 research papers in reputed international journals (SCI & Web of Science).